Modular Quadrotor MAVs

Vishal Vaswani, Samuel Loh*, Benson Tan and Kalenjit Singh, Sutthiphong Srigrarom
University of Glasgow Singapore

ABSTRACT

Historically, helicopters with four rotors (quad-rotors) have been very uncommon, mainly due to the fact that most of the common payloads could be lifted using one or two rotors. However, the quad-rotor possesses some special characteristics that make it attractive. One would be the superior payload capacity. Two, is the simplicity of the control system: the absence of complex rotor mechanisms and just by independently adjusting the speed of each rotor it is possible to control both the attitude and the horizontal/vertical motion. This system is particularly suitable for small unmanned aerial vehicles (UAV), because it reduces the complex mechanism of the rotors (saving volume and weight) and simplifies the control algorithms required for stable, untethered flight. Although much progress has been made in the field of quad-rotor UAVs, it is still a great challenge to build a quad-rotor capable of fully autonomous flight. Before the decision of appropriate control algorithms, it is essential to have complete understanding of quad-rotor dynamics and equation of motion. This technical paper presents a detailed quad rotor model design as well as the detailed algorithm for the control system. An ANSYS flow simulation was carried out on the modular structure of the quad rotor. Different sensors were integrated with the control system to improve the stability and to reduce the pilot's workload. Its capabilities will be enhanced with semi-autonomous and autonomous functions that were implemented with the usage of GPS.

1. INTRODUCTION

A quad rotor is a rotorcraft equipped with four rotors laid up symmetrically around its centre. It is capable of hover flight, forward flight and vertical take-off and vertical landing. Therefore it is classified as a rotary-winged VTOL aircraft. Traditionally, the quad-rotor configuration is not of mainstream use in the aerospace industry, mainly because the usual payloads could be lifted using one or two rotors.

Much progress has been made in the field of quad-rotor UAVs; it is still a challenge to build a quad-rotor capable of stable, untethered flight with fully autonomous capabilities. Semi-autonomous capabilities will include safe low level flight and navigation in an urban environment. In order to enable this quad-rotor to fly autonomously, several controllers have been considered. It is expected that these controllers will be tested in the model before implementing them in the actual rotor-craft. To do so, it is necessary to implement the appropriate control algorithms and to have a suitable set of on-board sensors. As for the design of the control algorithms, in order for it to be successful and stable, it is essential to have a complete understanding of quad-rotor flight dynamics.

*E-mail address: samuelohyk@gmail.com

2. QUAD ROTOR CONTROL

The configuration consists of two clockwise rotating rotors and two counter clockwise rotating rotors to compensate for the torque produced. The placement of the rotors can be seen in figure 1.

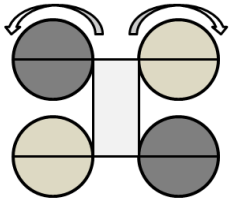

Figure 1: Control for H Frame Configuration

This unconventional design does not require a cyclic and collective pitch control mechanism of a conventional helicopter. Instead, each motor RPM is varied to replicate the exact controls of a conventional helicopter.

To increase its altitude, all four motors will increase to the same RPM. To pitch forward, the aft two motors are required to increase in RPM, while the forward two motors will have a slight decrease in RPM. Hence, a nose down or forward pitch attitude is produced about the *x*-axis and vice versa for pitch up attitude. This methodology of pitch can be used for roll about the y-axis as well. To yaw right, the clockwise rotating motors will increase in RPM and vice versa for yawing left. However, before designing the model of a quad rotor, quad rotor dynamics must be further explored.

3. QUAD ROTOR DYNAMICS

Quad rotor dynamics will include the equations of motion along all three axes. The force, moments and thrust equations are vital when designing a quad rotor. The general equations of motion can be written by considering various variables namely, force, moment of balance, moment of inertia and drag coefficients C_d. A fixed frame of body will be assumed to be at the center of gravity of the quad rotor with the z-axis pointing up. This body of axis is directly related to the three Euler angles ψ, θ, ϕ representing roll, pitch and yaw respectively. C_{d1} to C_{d6} are independent drag coefficients for the three body axes and the Euler angles.

$$\ddot{x} = \frac{F_{total}(\cos\psi \sin\theta \cos\phi + \sin\phi \sin\psi) - C_{d1}\dot{x}}{m} \quad (1)$$

$$\ddot{y} = \frac{F_{total}(\sin\psi \sin\theta \cos\phi - \cos\psi \sin\phi) - C_{d2}\dot{y}}{m} \quad (2)$$

$$\ddot{z} = \frac{F_{total}(\cos\psi \cos\phi) - mg - C_{d3}\dot{z}}{m} \quad (3)$$

$$\ddot{\phi} = \frac{l(-F_1 + F_2 + F_3 - F_4) - C_{d4}\phi}{j_1} \quad (4)$$

$$\ddot{\theta} = \frac{l(-F_1 - F_2 + F_3 + F_4) - C_{d5}\theta}{j_2} \quad (5)$$

$$\ddot{\psi} = \frac{l(F_1 - F_2 + F_3 - F_4) - C_{d6}\psi}{j_3} \quad (6)$$

Assuming the initial condition of the model is in a low speed flight; drag is assumed to be negligible hence zero. Input equations are defined as:

$$U_1 = \frac{F_1 + F_2 + F_3 + F_4}{m} \quad (7)$$

$$U_2 = \frac{-F_1 + F_2 + F_3 - F_4}{m} \quad (8)$$

$$U_3 = \frac{-F_1 - F_2 + F_3 + F_4}{m} \quad (9)$$

$$U_4 = \frac{F_1 - F_2 + F_3 - F_4}{m} \quad (10)$$

U_1 represents total thrust acting on the body in the z-axis. U_2 and U_3 are the pitch and roll inputs respectively. U_4 is the yawing moment. Using actuator disc theory, advance ratio and coefficient of thrust formulas, the thrust equation can be formulated.

Advance ratio: $$J = \frac{V}{nD} \quad (11)$$

where, D is the rotor diameter, V is the velocity and n is the rotor's rotational speed.

With the definition of coefficient of thrust:

$$T = C_T p n^2 D^4 \quad (12)$$

The values of advance ratio (J), coefficient of thrust (C_T) may be selected from the datasheet of propellers [2].The center of gravity is assumed to be at the middle of the frame. A lower center of gravity will ensure a less sensitive angular acceleration. The tilting forces towards the center will reduce the pitching and rolling moments and vertical thrust. Hence, this results in an increase in static stability.

Although complex control mechanisms were eliminated, the quad rotor is a rotor winged craft and susceptible to the same aerodynamic effects as a conventional helicopter.

4. AERODYNAMIC EFFECTS

The quad rotor is modelled as a rotor winged aircraft. As such, it is subjected to various aerodynamic effects as a conventional helicopter would. It is however, possible to mitigate certain aerodynamic effects and at the same time to enhance flight performance.

Ground effect influences rotor operations close to the ground. There are two types of ground effect: In Ground Effect and Out of Ground Effect. In Ground Effect usually occurs less than one rotor diameter above the surface of the ground. As the induced airflow passing through the rotor disc is reduced by the surface friction, the lift vector increases. This allows a lower rotor blade angle for the same amount of lift, which reduces induced drag. In Ground effect also restricts the generation of blade tip vortices due to the downward and outward airflow making a larger portion of the blade produce lift.

Ground effect occurs on all types of surfaces. It is at its maximum effect in zero wind conditions over a firm and smooth surface (runway). Tall grass, uneven terrain, water surfaces will alter the airflow pattern which cause an increase in rotor tip vortices. The formation of tip vortices will be mitigated in the quad rotor's structural design.

When the rotorcraft moves through the air, the relative airflow through the rotor disc is different on the advancing side than the retreating side as seen in figure 2.

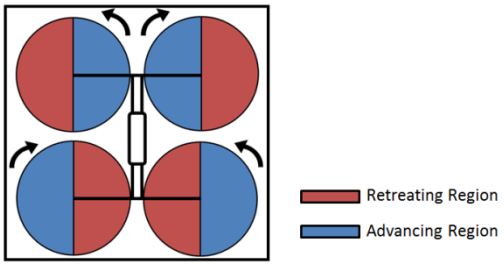

Figure 2: Advancing and Retreating Blade Regions [3]

The relative wind encountered by the advancing blade is increased by the forward speed of the helicopter. The relative wing speed acting on the retreating blade is reduced. Thus, the advancing blade produces more lift than the retreating blade. This phenomenon is known as Dissymmetry of Lift. This results in erratic pitching and rolling moments in flight. On a conventional helicopter, a horizontal hinge (flapping hinge) allows the individual rotor blades to flap as they rotate. [3] This unique system however, does not contain such a mechanical hinge. Instead, a complex control system will be implemented to reduce these unwanted moments.

5. STRUCTURE

A stable structure is required for testing aerodynamic effects associated with a rotor winged aircraft. In addition, a resilient and durable material will be a plus point as a

platform for a quad rotor system. In the market, there are numerous materials used in the design of a multi rotorcraft and three dimensional printing is increasingly popular due to its versatility. However, a revolutionary design that was manufactured by Safe Flight Copters LLC, in San Francisco, USA [4] focuses on the words 'modular' and 'safety'.The structural design is best understood as an eggshell concept or also known as monocoque. While hollow in the interior, the design and material used can contribute a huge factor in improving its durability and strength. The manufacturing process is done by plastic injection moulding in which a plastic polymer was pressed onto a mould. Carbon fibre rods reinforce the frame. The plastic polymer is specifically known as polyethylene terephthalate (PET). It is one of the most common types of polyester. Two monomers, known as ethylene glycol and purified teraphthalic acid are combined to form PET. PET has excellent wear resistance and has no centreline porosity. Typical properties of PET that are considered for this design are its tensile strength, tensile modulus, flexural strength, flexural modulus, dielectric constant, and dielectric strength [5]. A summary of the properties considered can be seen in table 2 of Appendix A.

This revolutionary design emphasises strongly on safety yet it is a modular design which is relatively rare in the market of multi rotorcraft. The modular concept essentially divides the quad rotor into parts. The parts consist of the lower fuselage & landing gear, upper fuselage, and two rotor modules as seen in figure 3.

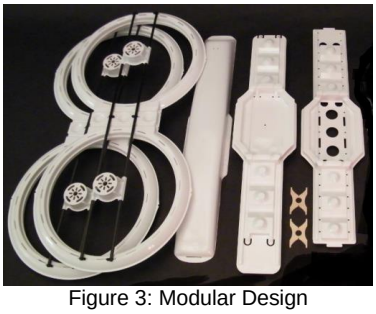

Figure 3: Modular Design

The design feature requires no metallic linkages to connect the parts. Four rubber bands and puzzle joints secures the pieces together instead. Redundancy has been considered in this design in which the modules will not come apart while maintaining stable flight performance even if two of the four rubber bands have snapped. The plastic frame is designed to flex and disengage upon an impact or a crash. Hence there is a huge reduction in assembly time and maintenance cost.

A reduction of propeller tip vortices improves propeller efficiency. In other words, the generation of lift by the propeller will require less power for a specific throttle setting with shrouds installed. Rotor operations generate a suction pressure on the inlet. This results in additional lift. The total thrust will be contributed by the rotor and the shroud. The overall thrust with the installation of shrouds for a given power input exceeds unshrouded rotors by about30% as seen in figure 4 below.

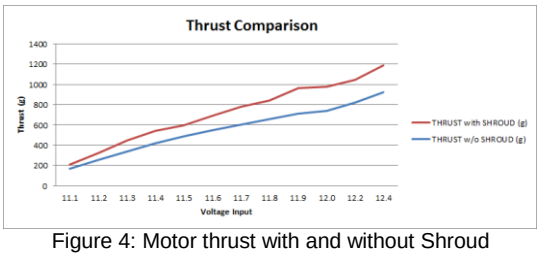

Figure 4: Motor thrust with and without Shroud

A slight increase in stability of hover flight was also observed. Propellers screen guards may also be installed as a first line of defence against foreign object debris that could stall a motor or damage the propeller in flight.

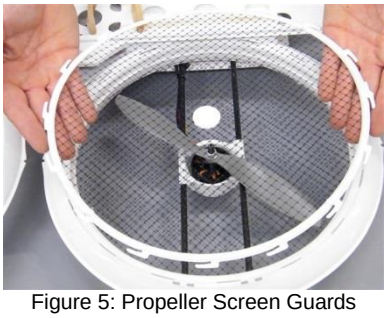

Figure 5: Propeller Screen Guards

The screen guards are made from polypropylene which is a thermoplastic polymer found in a variety of household products. The guards are resilient against foreign objects when tensioned by thermal appliances. However, installing a propeller screen guard also raised concerns of affecting the motor thrust. Using a tachometer and lining a reflective tape on the propeller, the individual motor RPM are as follows:

Throttle	Motor 1	Motor 2	Motor 3	Motor 4
50%	5700	5750	5725	5700
100%	11800	11850	11750	11850

Table 1: Screen guards installed

Throttle	Motor 1	Motor 2	Motor 3	Motor 4
50%	7050	7000	7020	7000
100%	13200	13100	13100	13200

Table 2: Screen guards removed

The simple tachometer test shows how the installation of screen guards reduces the thrust significantly by about 10%. This reduction of thrust is found to be acceptable performance losses for what is gained.

6. AVIONICS

The quad rotor is capable of both semi-autonomous flight (Pilot inputs/First Person View) and fully autonomous

capabilities. A general diagram of the avionics design on the quad rotor is shown in figure 6 below.

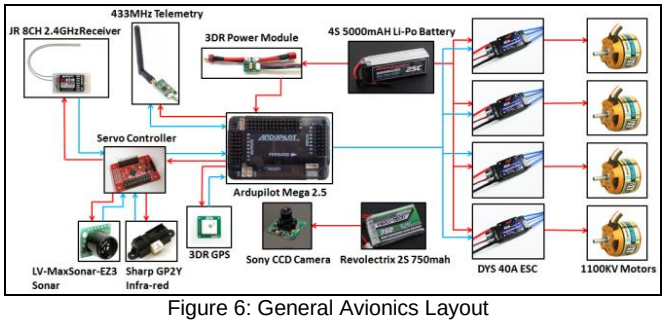

Figure 6: General Avionics Layout

Basic RC components consist of the brushless motor, propellers, electronic speed controller (ESC), lithium-polymer battery and an 8 channel transmitter/receiver. The list of components can be seen in table 5 of Appendix A. For the on board controller, an Atmel ATMEGA2560 microprocessor is used for processing information while an integrated barometer is used for high altitude sensing.

Based on the combination of weight of the components and weight of miscellaneous wires taken into consideration, the total weight of the rotor craft is estimated to be 1500 grams. The maximum thrust of each brushless motors produce with the chosen propeller is 1130 grams [6] with a size 10 propeller. A total of four motors will produce 4520 grams of thrust. The thrust to weight ratio would be 3:1. This amount of thrust is sufficient to propel the quad rotor and the capacity of the four cell lithium polymer (Li-Po) battery ensures flight endurance of 15 minutes after a flight test.

The propeller size was chosen due to the limitation of the propeller shroud design. A telemetry antenna operating at 433MHz ensures constant feedback of critical data such as current position to the ground station at all times.

During semi-autonomous flight, a servo controller has been integrated to regulate the radio signals from the receiver and signals of the implemented sensors. An ultrasonic sensor and infra-red sensors have been implemented in the system.

An ultrasonic sensor [7] enables altitude hold and autonomous take off/landing. The ultrasonic sensor functions in a similar principle to an aircraft's radar altimeter by taking reference to the datum. Atmospheric pressure is therefore negligible and the quad rotor will maintain set altitude regardless of sea level. The disadvantage of an ultrasonic sensor is it's only accurate on smooth surfaces at low altitude (15cm – 645cm). Carpet and irregular surfaces such as grass will interfere with the sensing capability and generate inaccurate distance readings. The servo controller essentially controls the amount of RPM the motors are required to generate to maintain altitude over time. In other words, the pilot is not required to control the throttle setting of the quad rotor. The graph below depicts the limitations of the sensor and also readings of the sensor. From the graph, is it observed that there is a 15 cm deadband.The height is registered once the quad rotor has moved out of the dead band. The altitude hold can be manually set or programmed. The pre-set altitude used will be 175 cm.The time scale does not reflect the trigger time. This graph plot depicts the flight envelope and the accuracy of the ultrasonic sensor while maintaining altitude.

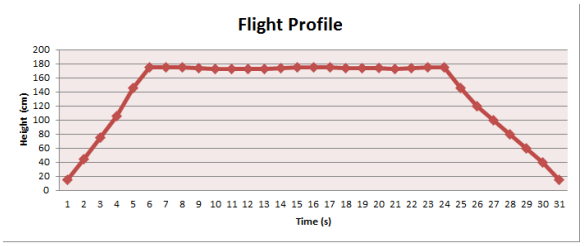

Figure 7: Ultrasonic Sensor readings

During the cruise phase, discrepancies in altitude readings can be observed. This is due to external disturbances from air-conditioning and pilot inputs.

An infra-red sensor has been implemented for obstacle & collision avoidance. The infra-red sensor's environmental perception is 25 centimeters with a quick trigger time of 50 milliseconds. An incremental corrective response has also been implemented. For every exponential increase of 5 centimeters, the servo controller will increase the respective motor RPM to accelerate the rate of correction.Below is a block diagram for the infra-red sensors operation.

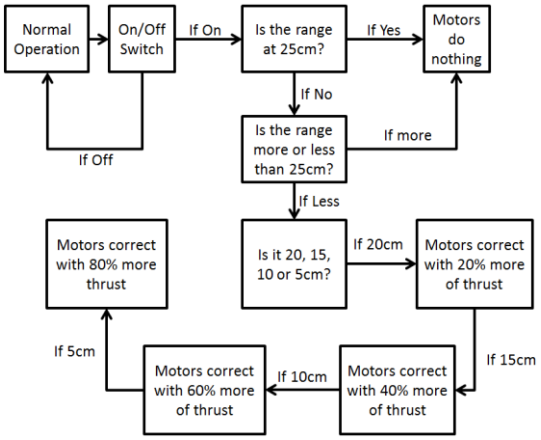

Figure 8: Obstacle & Avoidance System

The infra-red system and ultrasonic system can be removed and attached to interact with any Arduino based flight controller in the market. This is to prevent any discrepancies when the firmware or program in the fight controller has been updated. If required, the user may choose to remove the implemented sensors and install other types of sensors with the servo controller to enhance the capabilities of the quad rotor.

A charge-coupled-device (CCD) phase alternating lines (PAL) camera is used to capture images and provide video

feedback to the ground station. An independent two cell lithium polymer batterygenerates enough power for the camera to last up to a few hours, which is more than sufficient. The camera may be installed at the nose of the quad rotor which contains a servo to pan the view vertically. If preferred, an aft mount can also be used to install a camera for third person view.

Basic RC components and pilot inputs are insufficient for minute corrections. A complex control system must be implemented for auto stabilization along all 3 axes.

For any radio controlled aircraft, safety is paramount. Regulations require the aircraft to have failsafe on board in the event of a loss in data link. The controller has two types of failsafe. The first failsafe is the arm/disarm feature. After switching on the transmitter and connecting the battery, an arm sequence is required to send current to the brushless motors. Without this arming sequence, the motors will not spin even if the pilot decides to increase the throttle stick. The arming of the controller is achieved by pushing the yaw stick to the left for five seconds. This command will be input into the controller and the motors will be armed for flight. For landing, the user is required to push the yaw stick to the right for three seconds to disarm the motors. This failsafe function runs on the secondary PPM encoder processor.

The encoder also detects the loss of RC signal in the RC receiver and will initiate a user defined set of autonomous commands. These commands can range to loiter about the last known position, return to its initial starting point (Home) or perform an autonomous landing. This failsafe function will require calibration to the radio transmitter as well. The user needs to lower the throttle PPM value than the lowest stick position during the first binding of transmitter and receiver. This setting will tell the controller that this is not a user induced action but rather a loss of data link. Therefore, the controller will not initiate a user defined command when the pilot reduced the throttle stick to zero.

7. CONTROL

For auto stabilization along 3 axes, an inertial measurement unit (IMU) will be implemented into the system based on direction-cosine-matrix (DCM) [8]. The theory is to use gyro information as the primary link between the reference frames while using global positioning system (GPS) and accelerometer information to compensate for gyro drift.

The orientation of the aircraft can be described by three consecutive rotations, whose order is important. The angular rotations are called the Euler angles. The orientation of the body frame with respect to the fixed earth frame can be determined from equations (13) to equations (17) and can be seen in figure 15.

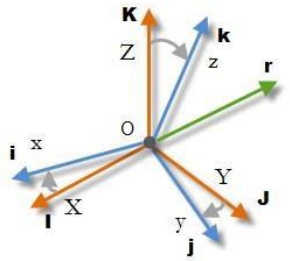

Figure 9: Orientation of Body to Earth coordinates

The transformation to a fixed body frame of reference from an inertial frame of reference (Earth) must be performed. Essentially, the transformation matrix requires three rotations about the *z* axis, *y* axis and finally the *x* axis.

$$R_z = \begin{bmatrix} \cos\psi & -\sin\psi & 0 \\ \sin\psi & \cos\psi & 0 \\ 0 & 0 & 1 \end{bmatrix} \tag{13}$$

$$R_y = \begin{bmatrix} \cos\theta & 0 & -\sin\theta \\ 0 & 1 & 0 \\ \sin\theta & 0 & \cos\theta \end{bmatrix} \tag{14}$$

$$R_x = \begin{bmatrix} 1 & 0 & 0 \\ 0 & \cos\phi & -\sin\phi \\ 0 & \sin\phi & \cos\phi \end{bmatrix} \tag{15}$$

$$R = R_z R_y R_x \tag{16}$$

$$R = \begin{bmatrix} c\psi.c\theta & c\psi.s\theta.s\phi - c\phi.s\psi & c\psi.s\theta.c\phi + s\phi.s\psi \\ s\psi.c\theta & s\psi.s\theta.s\phi + c\phi.c\psi & s\psi.s\theta.c\phi - s\phi.c\psi \\ -s\theta & s\phi.c\theta & c\phi.c\theta \end{bmatrix}$$

where, c = cosine and s = sine. (17)

The R matrix above contains all the information needed to express the orientation of the plane with respect to the ground. This matrix is also called the direct-cosine-matrix because each cosine angle is the angle between an axis of the aircraft and an axis on the ground. Electronic rate gyros rotate with the aircraft, producing signals proportional to the rotation rate. Since rotations do not commute and the sequence of rotations is important, the integration of gyro rate signals to obtain angles will not work. The kinematics of rotations must be looked into.

Rate of change of a rotating vector:

$$\frac{dr(t)}{dt} = w(r) \times r(t) \tag{18}$$

w(r) is the rotation rate vector.

By numerically integrating a cross product to track the rotating vector,

$$r(t) = r(0) + \int_0^t d\theta(t) \times r(t) \tag{19}$$

$$d\theta(t) = w(t)dt \tag{20}$$

$r(0)$ = starting value of the vector

$\int_0^t d\theta(t) \times r(t) =$ change in the vector

Equations (19) and (20) will be applied to the rolls and columns of Matrix R as rotating vectors. Ideally, the axes of the aircraft in the earth frame of reference will be tracked. Since the gyro measurements are made in the aircraft frame of reference, the symmetry in the rotation must be recognized. The earth axes can be tracked in the plane frame by flipping the sign of the gyro signals.

$$r_{earth}(t) = r_{earth}(0) + \int_0^t r_{earth}(t) d\theta(t) \quad (21)$$

$$d\theta(t) = w(t)dt \quad (22)$$

r_{earth} = one of the earth axis

The vectors in the above equations are the rows of Matrix *R* in equation (1.21). To implement this, the differential form of the above equations is:

$$r_{earth}(t + dt) = r_{earth}(0) + r_{earth}(t) \times d\theta(t) \quad (23)$$

Lastly, the correction rotation rate must be added that comes out of the proportional + integral drift compensation feedback controller, to the measurements made by the gyros to produce the best estimation of the true rotation rate.

$$w(t) = w_{gyro}(t) + w_{correction}(t) \quad (24)$$

$w_{gyro}(t)$ = three axes gyro measurements

$w_{correction}(t)$ = gyro correction

Even though the gyros functions well, the uncorrected offset of a few degrees per second must be cancelled. The rotation error vector can be fed back through a proportional plus integral (PI) controller to produce a rotation rate adjustment for the gyros. The derivative term may be used to improve stability.

Accelerometers are used for roll and pitch drift correction because they contain zero drift. Centrifugal acceleration will also be accounted for as the cross product of the gyro vector and velocity vector.

$$A_{centrifugd} = w_{gyro} \times V \quad (25)$$

$$V = \begin{bmatrix} velocity \\ 0 \\ 0 \end{bmatrix} \quad (26)$$

To estimate gravity that is adjusted for centrifugal acceleration, the centrifugal acceleration estimate must be added. Hence:

$$g_{reference} = Accelerometer + w_{gyro} \times V \quad (27)$$

$$Accelerometer = \begin{bmatrix} Accelerometer_x \\ Accelerometer_y \\ Accelerometer_z \end{bmatrix} \quad (28)$$

In addition to the reference measurement of gravity, estimation must be done based on the DCM. The roll and pitch rotational correction vector in the body frame of reference is computed by taking the cross product of the Z row of the DCM with the normalized gravity reference vector (Equation 27).

$$RollPitchCorrectionPlan = \begin{bmatrix} r_{zx} \\ r_{zy} \\ r_{zz} \end{bmatrix} \times g_{reference} \quad (29)$$

Gyros tend to saturate during tight turns. Actual acceleration might exceed the range of the accelerometer. This can be avoided by adding gyro terms in the feedback controller to limit the turning rate.

In a nutshell, the laws of DCM depict the controller to use gyro information to integrate the time rate of change of the direction cosines. Speed and gyro information are used to adjust accelerometer information for centrifugal effects. 3 axis accelerometers information are used to cancel roll and pitch drift. Lastly, GPS information will be utilised to cancel yaw drift.

A proportional-integral-derivative (PID) controller is a control closed loop feedback system. The PID controller calculates the error value as a difference between the measured value and a desired set point. The comparison is then multiplied times Rate P. The PID will ensure the commanded rate matches the actual rate from the gyro. Values will then be subsequently converted into Pulse Width Modulation (PWM) and set to the motors via the ESCs.

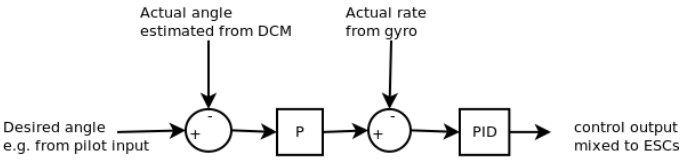

Figure 10: PID Control Diagram

Increasing Proportional gain will increase the rotation rate as desired to correct any errors. A greater value will result in a faster attempt to achieve the desired attitude. However, an exceptionally high value will result in the correction of pilot's input almost immediately which is considered undesirable. Integral term can be used to account for weak motors or strong external forces. Again, if the value is too high, oscillations will be observed. Derivative term in the system will predict behaviour and improve settling time and overall stability. The final results for the PID values are:

Rate_P = 0.170
Rate_I = 0.650
Rate_D = 0.008

PID controllers however, are insufficient for fully autonomous flight. An additional component must be implemented.

8. MAN-MACHINE-INTERFACE

A first person view (FPV) camera has been implemented to provide real time video feedback to the ground station or pilot. A split screen will be required to display video and air data. But this set up can be drastically improved by using the video display to replace the artificial horizon as a heads up display (HUD) through graphic user interface (GUI). This combination of GUI and FPV is as shown in figure 11 below.

Critical air data would include an artificial horizon, airspeed, altitude, heading, mode of flight, battery voltage and capacity. This integration improves pilot's situational awareness and reduces the pilot's workload during semi-autonomous flight. In addition, the video can be recorded at any point of time to be used for analysis if needed.

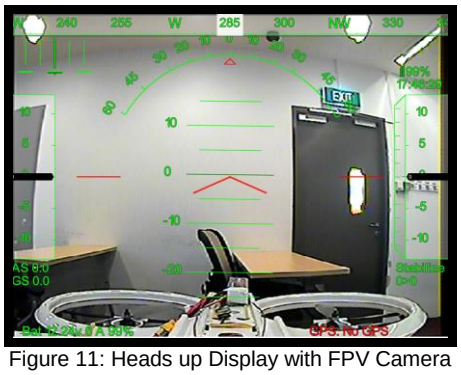

Figure 11: Heads up Display with FPV Camera

9. AUTONOMOUS FLIGHT

To achieve outdoors autonomous flight, a GPS module can be implemented with the controller.

Figure 12: 3DR GPS Module

Most GPS receivers are using pseudorange data available on the GPS L1 channel of 1675.42MHz. Optimally, the receiver receives satellite based augmentation system (SBAS), differential global positioning system (DGPS) corrections which give meter precision. However, an advanced and expensive method can provide centimeters or even millimeters of precision. These GPS receivers uses the previous method as mentioned and at the same time with carrier phase smoothing, carrier phase corrections or Real Time Kinematic (RTK) as well as L2 channel semi-codeless tracking of 1227.60MHz. RTK uses pseudorange to compute position and at the same time, Doppler measurements and carrier phase smoothing. The base station collects these data and transmits them to the receiver on the quad rotor. Since the base is on a known coordinate, computations can go up to millimeters accuracy.

In addition, these account for real time local ionospheric corrections which provide pin point accuracy.

GPS may be accurate for the outdoors autonomous flight, but a problem known as multipathing causes GPS position errors [9]. This problem is difficult to detect and compensate but through understanding, they can be avoided. Multipathing results when the direct path to the receiver is reflected by an object. The reflecting surface may be from buildings, mountains, trees and even the human body. A radio reflector at 1.6GHz can also cause multipathing. When the path is blocked, the radio signals have to travel further to get to the receiver than they should. The GPS will miscalculate its position because the signals have travelled further than a direct line of sight as in figure 13 below.

Ionospheric perturbations and magnetic storms can cause signal delays as well. This is partially compensated using SBAS and L1/L2 decoding receivers. A general rule of thumb for autonomous flight using GPS would be to fly with clear sky view and no obstructions.

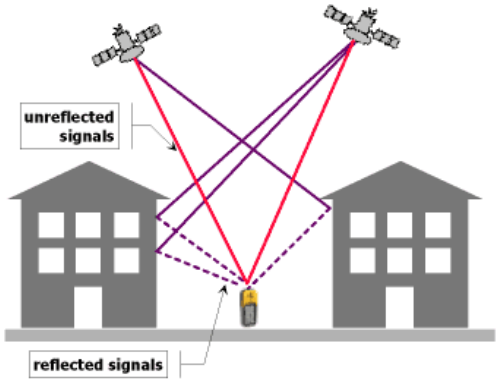

Figure 13: GPS Multipathing

Figure 14: User Interface for GPS way points

A utility tool known as Mission Planner can be used as an interface in conjunction with the Ardupilot Mega 2.5

controller. This tool interacts with the controller which enables the user to insert or select GPS coordinates, and set them as way points for the quad rotor to fly.

A GPS failsafe has also been incorporated. This GPS failsafe event will occur if the GPS position "glitches" while the quad rotor is in autonomous GPS mode. A projected path and GPS reported path will be relayed to the controller. The projected position will be based on the previous GPS position and velocity. GPS position "glitches" are detected by comparing each new position update (every three seconds) received from the GPS with a position projected out from the previous position and velocity. A radius around a way point can be set to allow positions within the area to be accepted. The radius can range from 5 meters to 10 meters. Once within the radius, the controller "accepts" the new position and the cycle repeats. If the GPS position updates outside the boundary of the projected and acceptable radius, it triggers a user defined GPS failsafe command after five seconds. Manual radio control via a pilot can also be utilised in such a situation.

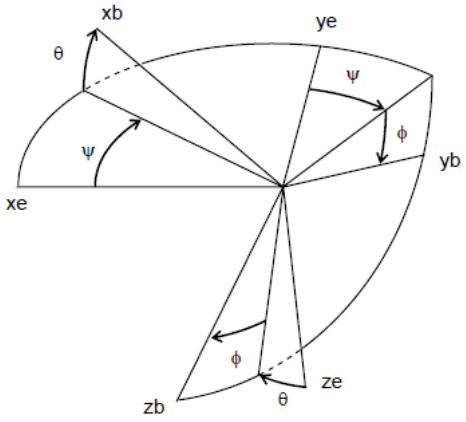

Figure 15: Body to Earth frame of reference

10. CONCLUSION

The aim of this project was to have a fully functional quad rotor capable of semi-autonomous control and autonomous flight. During test runs, we achieved perfect stable flight and autonomous functions while exhibiting visible corrections from the controller. The physical structure is successful both in terms of weight, strength and durability. The final weight was measured to be 1800 grams. Fully functional software was implemented for the control of the four motors on a commercially available microcomputer and obtained excellent results with an oscilloscope set up to compare and read operator inputs & PWM inputs. The autonomous aspect of the project was also successful. Fully autonomous functions were observed without the intervention of the pilot aside from monitoring of flight. Future developments would include fine tuning of the controller and outfitting with LiDAR (Light Detection And Ranging) [10] for precise autonomous indoors navigation. Structural enhancements such as a retractable landing gear and aerodynamic body can also be looked into.

References

[1] Leishman, G., *Basic Helicopter Aerodynamics*, Cambridge University Press, 2003.

[2] Norris, D. *Build your own Quadcoptor*, McGraw-Hill, 2014.

[3] Federal Aviation Administration, *Helicopter Flying Handbook*, Chapter 5 – Helicopter Components, Sections, and Systems. 2012.

[4] Ananda G., University of Illinois, Department of Aerospace Engineering, Propeller Database 2014: [ONLINE] Available at: http://aerospace.illinois.edu/m-selig/props/propDB.html

[5] Federal Aviation Administration, *Rotorcraft Flying Handbook*, Chapter 5-4 Main Rotor System. 2000.

[6] Safe Flight Copters LLC, San Francisco, California, United States of America: [ONLINE] Available at: http://safeflightcopters.com/SFC4410

[7] Plastic Properties INC, Bessemer City, North Carolina, United States of America. PET Properties [ONLINE] Available at:http://www.plastic-products.com/part12.htm

[8] Hobbyking, Turnigy D2836/8 1100KV, Brushless Motor datasheet, 2014. [ONLINE] Available at: http://www.hobbyking.com/hobbyking/store/uh_viewitem.asp?idproduct=18969

[9] Maxbotix LV-Maxsonar EZ-3 Ultrasonic Sensor Datasheet, 2012. [ONLINE] Available at: http://www.maxbotix.com/documents/MB1030_Datasheet.pdf

[10] Direct Cosine Matrix, Starlino Electronics, 2011. [ONLINE] Available at: http://www.starlino.com/dcm_tutorial.html

[11] Joe Mehaffey, GPS Multipathing, 2013. [ONLINE] Available at: http://gpsinformation.net/multipath.htm

[12] National Oceanic and Atmospheric Administration, Light Detection And Ranging (LiDAR), 2013. [ONLINE] Available at: http://oceanservice.noaa.gov/facts/lidar.html

APPENDIX A: DATA

Components	Description
Controller	Ardupilot Mega 2.5
Electronic Speed Controller	Dys 40A Programmable ESC
Brushless Motor	Turnigy 1100KV
Propeller	APC 10 by 4.7
Global Positioning System	3DR GPS Module
Infra-red Sensor	Sharp GP-2Y
Ultrasonic Sensor	LV-Maxsonar-EZ3
Battery	14.8 4S 5000mAH Li-Po
Camera	CCD Camera
Transmitter/Receiver	JR 8 channel TX/RX
Wireless Data link	3DR 433MHz Radio Telemetry

Table 3: Summary of Components